# Automation of Temperature Measurement in Induction Motors of Hermetic Compressors Based on the Method of Temperature Rise by Resistance

Murilo F. Vitor ⬤ , João P. Z. Machado ⬤ , Antonio L. S. Pacheco ⬤ , and Rodolfo C. C. Flesch ⬤ , *Member, IEEE*

*Abstract*—Recent studies have proposed the use of artificial neural networks to establish a correlation between the cooling capacity of refrigeration compressors and the results of quick production quality tests. However, the temperature measurement method used in the tests reflects a high uncertainty in the estimated performance parameters, primarily because the measurement is performed on the compressor shell, which has large thermal inertia and does not accurately reflect the temperature changes observed during the tests. This study proposes a set of modules that allow the application of the method of temperature rise by resistance to estimate the winding temperature of the single-phase induction motor of the compressor in quick quality tests. The winding temperature is a better estimate of the temperature at which the refrigerant fluid enters the compression cylinder and its use solves many of the problems associated with the traditional method. Validation tests show that the proposed solution is capable of automating the measurement in a safe, agile, and metrologically more reliable manner than the method currently used in quick quality tests in the industry.

*Index Terms*—Compressors, cooling capacity, electrical resistance measurement, single-phase induction motors, temperature measurement, temperature rise by resistance.

## I. INTRODUCTION

**O**ne of the most important parameters to characterize the performance of a refrigeration compressor is its cooling capacity (CC) [1], which is a measure of the capacity of a compressor to generate mass flow of the refrigerant fluid under specified operating or test conditions [2]. CC measurements are used for both quality control and research and development activities [3]. The equipment required to obtain CC in a single compressor requires specialized instrumentation, which results in a high cost for each test position. Furthermore, the time required for tests to obtain such a parameter using traditional test rigs is long, typically over three hours. Consequently, a small number of samples of compressors are tested, which introduces a delay of hours between the occurrence of a performance problem and its detection [4].

Murilo F. Vitor and João P. Z. Machado are with Laboratório de Instrumentação e Automação de Ensaios, Universidade Federal de Santa Catarina, Florianópolis, Brasil (e-mail: murilo.vitor@labmetro.ufsc.br; joao.zomer.m@posgrad.ufsc.br).

Antonio L. S. Pacheco is with Instituto de Eletrônica de Potência, Universidade Federal de Santa Catarina, Florianópolis, Brasil (e-mail: pacheco@inep.ufsc.br).

Rodolfo C. C. Flesch is with Departamento de Automação e Sistemas, Universidade Federal de Santa Catarina, Florianópolis, Brasil (e-mail: rodolfo.flesch@ufsc.br).

As a result of efforts to reduce testing time, literature lists approaches that consider correlated quantities obtained from other tests with short duration to infer CC, such as the artificial neural network (ANN) ensemble proposed in [3] and improved in [5] by modifying the test rig to measure certain quantities, to avoid the need for information about the design parameters of the compressor under test. This approach enables the determination of the CC of all compressors produced using the information obtained from quick quality tests performed in the production line, called pressure rise tests (PRTs), after being processed by an ANN, in approximately 0.05% of the time required by traditional methods. The input parameters used by the ANN are the pressure rise rate (PRR), the electrical power consumed (consumption), and the compressor shell temperature. In addition, a formalization of the method for evaluating the uncertainty of the inference is proposed in [6] and it shows that the temperature uncertainty plays an important role in the overall test result uncertainty, which is about $\pm 6\%$ of the inference value, while in traditional tests this value is about $\pm 3\%$ of the reading.

In addition to the uncertainty associated with the temperature measurements themselves, the point at which the temperature is measured affects the overall inference uncertainty. The ideal method would be to measure the compressor motor winding temperature instead of the shell temperature, since the former better represents the temperature at which refrigerant enters the compression cylinder [7]. Due to the production line layout and the short test length, there is not enough time for the homogenization between the shell and internal temperatures, so the shell temperature does not correspond to the temperature of interest. Also, since the compressors tested are hermetic, the direct measurement of the motor winding temperature is quite challenging. Given this limitation, a promising approach is the indirect measurement of the temperature of the single-phase induction motor (SPIM) of the compressor.

There are several methods for indirectly estimating the temperature of induction motors in literature, and most of them are designed to obtain the estimates while the motor is in operation. Those methods are more susceptible to noise and interference than a direct measurement approach, so it is natural that their estimates have a relatively large uncertainty value for some applications [8]. Indirect measurement methods can be categorized into three broad types: thermal model, machine parameter, and the combination of both [9]. Thermal models have been widely used in thermal protection, but the

expected estimation error for this type of method is in the order of $2\,^{\circ}$C [10]. A recent method described in [11] was able to obtain estimation errors significantly smaller than $2\,^{\circ}$C, but the characterization of machine parameters are infeasible in a production line. Thermal models can also be combined with electrical models, so that an electrical resistance value is estimated based on measured machine parameters and then translated into a temperature estimate. This method tends to be more robust to changes in operating conditions, but the expected error is equivalent to that presented by thermal model-based methods [12]. The machine parameter approach relies on resistance estimation to calculate temperature, being divided into model-based estimation and signal-injection estimation, with the latter being the preferred method in the literature [9]. Again, the estimation errors reported in the literature have an order of magnitude of some degrees Celsius, both for the alternate current [13] and direct current [14] methods. In addition, model-based methods require prior characterization of motor parameters, which is not feasible in a production line.

An approach to obtain the temperature of interest with an acceptable uncertainty value is the method of temperature rise by resistance (TRR), as described in [15]. To use this method, the measurement procedure should be started immediately after the test has ended [16]. However, because the time for the initial measurement may vary due to safe working practices, terminal reaching, and operator variations, the resistance at the time instant when the motor is turned off is usually not obtained, and extrapolation backward must be used to obtain this value [17]. A switching device was proposed in [18] to compare different extrapolation methods, showing that the measuring error is inversely proportional to the length of the time window for the first resistance measurement. The best test scenario reported in [18] shows a standard uncertainty of $0.4\,^{\circ}$C, which corresponds to an expanded uncertainty of $0.8\,^{\circ}$C. This uncertainty is almost one order of magnitude smaller than that of other indirect estimation methods from literature and was defined as the target for this study. The proposed method achieved an expanded uncertainty of $0.4\,^{\circ}$C, even smaller than that obtained in [18].

The method proposed in [5] admits the temperature measurement at the end of PRT after the compressor is shut down. However, lack of synchronization between measurement and the test may affect the resistance measurement or damage the measuring instrument (e.g., ohmmeter or an association of voltmeter and ammeter). This study proposes a solution to ensure that the measurement process is automatic, occurs as soon as possible, and guarantees the safety of the operator, compressor under test and the measuring instrument, which in this work is an ohmmeter. Additionally, an uncertainty evaluation was performed to compare the uncertainty of the proposed method with that of the former measurement method for the PRT.

This paper is divided into five sections. The temperature measurement in the PRT is described in Section II. Section III presents the proposed set of modules, with their functionalities and particularities. The validation and evaluation of the module functions are presented in Section IV. In Section V the main conclusions of this study are presented.

## II. TEMPERATURE MEASUREMENT IN PRT

The PRT is a common way of assessing hermetic compressor quality in companies with high production flow. Because of its quick assessment, typically performed in less than $7\,$s, the test can be used to evaluate the functionality of each compressor produced. In the typical test configuration, the suction terminal of the compressor under evaluation is open to the environment and the discharge terminal is coupled to a pressure vessel of known volume. The compressor increases the pressure in the vessel by itself for a short time, which is used to measure the PRR [5]. In addition, the consumption of the compressor and the shell temperature are measured.

The PRT is usually performed as the last stage of a compressor assembly line. In some situations, the measurement is done right after the drying of the shell paint in a stove, resulting in a large temperature variability caused by the stove operation in batches and the different times for each compressor to reach the test station. However, both PRR and consumption are strongly affected by the compressor temperature. The PRR decreases as the temperature is increased, as a direct effect of the decrease in the density of the vapor at the inlet of the compression cylinder, thus resulting in a smaller amount of vapor being pressurized at each compression cycle [19]. The effects of temperature change in the consumption are also significant, since the temperature changes the resistivity of the conductors in the motor of the compressor. Due to the hermetic characteristic of the compressors, the internal temperatures cannot measured directly, so the shell temperature is measured and used to compensate for part of those changes, as discussed in [5].

Under normal conditions, the variations in motor winding resistance before the test occur mainly due to drying process in the stove and changes in the ambient temperature. During the test, the winding experiences the effects of the starting transient, in which the electric current is higher than that observed in steady state. Consequently, the dissipated electrical power increases with the square of the current, heating the winding resistance [20]. Currently, even if the temperature measurement was carried out immediately after the test, the effects of the motor operation would not reflect in the compressor shell temperature, due to the limited amount of time.

The authors in [5] identified good correlation levels between the PRT data and CC values, which are measured in laboratory. Based on this finding, the authors proposed a tool which makes use of PRT results and an ANN to make inferences of both the CC and its corresponding measurement uncertainty. The ANN-based tool uses as inputs the measured PRR, consumption, and shell temperature. In this case, in particular, using the motor winding temperature should be much more effective from the point of view of the desired modeling. Similarly, if the measurement uncertainty is reduced, the resulting inference uncertainty is reduced too.

The seminal work of Summers [21] shows that the TRR method provides accurate and consistent results of the average winding temperature of a motor, which is less prone to be affected by hot spots than temperature transducers. With this method, the main winding temperature of the stator of a SPIM

can be estimated by observing its electrical resistance variation between the measurement time and a known temperature condition [10]. This ratio can be described as [15]:

$$T = T_0 + (R - R_0)/(\alpha R_0), \qquad (1)$$

where $T$ is the stator main winding temperature; $T_0$ is the reference temperature; $R$ is the stator main winding resistance; $R_0$ is the resistance at $T_0$; and $\alpha$ is the temperature coefficient, which is a thermal property of the conductive material used in the main winding. The known temperature condition, characterized by $R_0$ and $T_0$, can be obtained either from tests in the stator manufacturing line or from resistance measurements of the compressor after a period of thermal equalization. The main winding is bigger and more distributed inside the stator, so it exchanges more heat with the inner part of the compressor. Also, since different models of compressors use different types of starting systems, it is difficult to standardize the measurements in the auxiliary winding. As a consequence, the better choice is to measure the main winding resistance.

The measurement of the main winding electrical resistance, $R$, must be made immediately after the compressor motor is switched off, so the temperature of interest takes into account the heating that happens in the motor operation during the test. However, the measurement of $R$ must be done after the main winding current is reduced to a safe value, since a large current can affect the measurement result and also damage the measurement system. It is also necessary to guarantee that the changes introduced by the measurement system, such as the lead wires, do not affect the proper operation of the motor nor the measured value for $R$, which can be done by using a four-wire configuration. Finally, the measurement system must eliminate the influence of the electrical devices typically associated with the compressor.

## III. PROPOSED SOLUTION

The proposed solution for obtaining the main winding temperature of the compressor is based on the indirect measurement of the temperature with low uncertainty by measuring $R$ of the SPIM of the compressor. A set of modules was developed to be used between the compressor electrical connection and the ohmmeter, which is used in a four-wire configuration, removing the wires influence from the measurement. The set of modules is controlled using the same computer and software that runs the PRT, ensuring synchronization between test execution and measurement, providing safety and automation to the process.

The three modules of the proposed solution are described individually in Sections III-A, III-B, and III-C, and were combined on an electronic board. Section III-A presents the Decoupling primary circuit, responsible for the automatic control of the operation states during motor testing. Section III-B presents the Relay logic safety circuit, which is responsible for adding an extra safety layer to the Decoupling primary circuit. Section III-C presents the Unloading check circuit, which is responsible for ensuring that the ohmmeter is enabled only after the motor main winding is at a safe voltage level.

### A. Decoupling Primary Circuit

The measurement of $R$ must occur at the end of the PRT, and to avoid that any energy accumulated in the motor affects the resistance measurement or eventually damages the ohmmeter, it can only be used when the main winding is discharged. For this reason, a discharge resistor is provided in the system. Another requirement for proper measurement is that neither the auxiliary elements (such as the thermal protector, starting system, and auxiliary winding circuit) nor the proposed circuit affect the measurement, so the auxiliary elements must be decoupled when needed. As an extra safety measure, the ohmmeter must be inserted into the circuit only when necessary.

The decoupling primary circuit, presented in Fig. 1, was designed to meet the requirements listed above. Its operation is based on the activation of relays, which act to switch parts of the circuit. The activation of these relays is performed using transistors. All the circuits with transistors have pull-down resistors to ensure the correct state when the base is left open. The elements for the activation of relays are not shown in the diagrams for the sake of simplicity.

The relay named Comutator (supplied by $V_1$ and activated by $V_{0_1}$) switches the compressor motor connection between the power supply and the discharge resistor. This module was designed so that in case of errors regarding the relays activation, the main winding is connected to the discharge resistor and not to the power supply. The Decoupler relay (supplied by $V_2$ and activated by $V_{0_2}$) ensures that auxiliary elements are disconnected during the measurement, and the Sectionalizer relay (also supplied by $V_2$ and activated by $V_{0_2}$) ensures that the element connected to the Comutator relay (power supply or discharge resistor) is disconnected during the measurement. Both the Decoupler and Sectionalizer relays are normally open for safety reasons, and it is necessary to activate them to start the compressor. The measurement of $R$ is performed with deactivation of the Decoupler and Sectionalizer relays, and the activation of the Measuring relays (supplied by $V_3$ and activated by $V_{0_3}$), which connect $R$ to the ohmmeter through a four-wire connection.
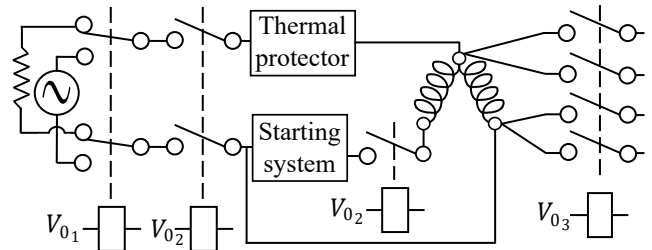


Fig. 1. Decoupling primary circuit, responsible for connecting the motor to the ohmmeter and removing unwanted elements during measurement.

Table I shows all the measuring system states (MSS) obtained by combining the states of the decoupling primary circuit relays. The states of interest are highlighted in bold and the other states can be considered as commutation errors that must be avoided. The Errors 1, 3, and 4 may cause either

a wrong measurement or an overvoltage condition, which has strong potential to damage the ohmmeter. Error 2 characterizes a non problematic state, because the measuring relays are not activated.

TABLE I
MSS ASSOCIATED WITH THE PRIMARY CIRCUIT.

| $V_{0_1}$ | $V_{0_2}$ | $V_{0_3}$ | MSS |
|---|---|---|---|
| 0 | 0 | 0 | **Motor disabled** |
| 0 | 0 | 1 | **Motor ready to measure** |
| 0 | 1 | 0 | **Motor unloading** |
| 0 | 1 | 1 | Error 1 |
| 1 | 0 | 0 | Error 2 |
| 1 | 0 | 1 | Error 3 |
| 1 | 1 | 0 | **Motor on** |
| 1 | 1 | 1 | Error 4 |

### B. Relay Logic Safety Circuit

The relay logic safety module was developed to prevent unwanted states from occurring, which would characterize the errors shown in Table I. This module serves as an extra layer of hardware protection which prevents improper triggering of the relays to produce error states, so even if the command signals are given, the relays will not be activated. The proposed solution consists in switching between supplying or not $V_1$, $V_2$, and $V_3$, which are responsible for supplying the Comutator, Sectionalizer, Decoupler, and Measuring relays.

The circuit is detailed in Fig. 2. The arrangement of the relays in the safety circuit excludes the states which satisfy the Boolean expression $V_{0_3} \cdot (V_{0_2} + V_{0_1})$, i.e. Error 1, Error 3, and Error 4. The state Error 2 is not excluded since it is not a state that may cause damage to the ohmmeter or the motor. In this case, $V_1$, $V_2$, and $V_3$ become outputs, which are functions of the states defined by $V_{0_1}$, $V_{0_2}$, and $V_{0_3}$.
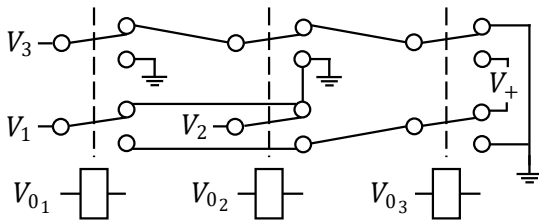


Fig. 2. Relay logic safety circuit, responsible for removing unwanted combinations of relays.

### C. Unloading check Circuit for Safe Voltage

The proper use of the modules presented in Sections III-A and III-B is sufficient to ensure the measurement of resistance with additional safety. However, the user could still command the start of the measurement without unloading the motor main winding. Therefore, a third circuit was designed to ensure that the measurement system is only enabled when the motor main winding is already at a safe voltage level. This third layer of protection was designed to prevent any external voltage that may affect the resistance measurement
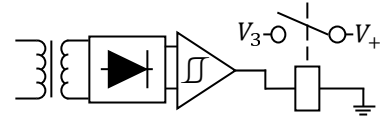


Fig. 3. Unloading check circuit, responsible for enabling the measurement at a safe voltage.

or damage the measuring instrument. The unloading check circuit is presented in Fig. 3.

The activation of this unloading check circuit is based on the comparison between the voltage over the Comutator terminals and a selected reference value. In this way, the voltage on the motor main winding is constantly monitored to know when the measurement is safe to happen. The unloading check circuit consists of a transformer, a rectifier bridge, and a comparator circuit. The isolation transformer is used to ensure that the monitored voltage is isolated from the reference voltage. A precision rectifier bridge was selected for its low voltage drop compared to a conventional rectifier bridge, and, together with a low-pass filter, is used to rectify the waveform for the comparator circuit. The comparator circuit has hysteresis to avoid unwanted switching caused by measurement noise, and its output activates a relay, interrupting $V_3$ or allowing it to supply the Measurement relays.

## IV. RESULTS AND DISCUSSION

The test rig shown in Fig. 4 was built to evaluate and validate the proposed solution. It contains an NI USB-6210 data acquisition board (DAQ) to control the relay states, an Agilent 34972A LXI data acquisition system with a 34901A multiplexer module used as ohmmeter to measure both the winding and Pt100 resistances, a Tektronix TDS 1002B oscilloscope to measure the dynamic signals, and a Heraeus B5050 F oven to simulate the drying oven from the assembly line. The automated test routine was developed in LabVIEW. Section IV-A describes the validation tests with regard to safety aspects. In Section IV-B, resistance measurements are evaluated with and without the proposed solution to show that it does not affect the result of the electrical resistance measurements. Furthermore, the conversion of the obtained resistance values in terms of the temperature values with their associated uncertainties is presented. Section IV-C describes the tests performed to evaluate the steady-state error between the TRR method and the winding temperature measurements.
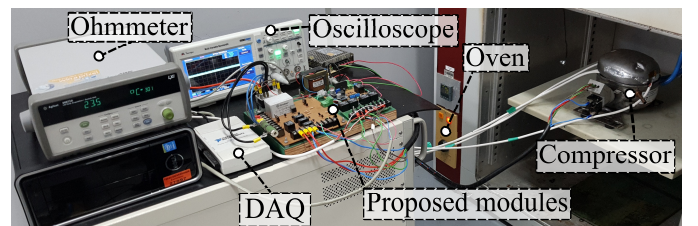


Fig. 4. Test rig assembled to evaluate the proposed modules.

## A. Validation Tests of the Proposed Modules

First, it was checked that the set of modules respects the Boolean expression $V_{0_3}.(V_{0_2} + V_{0_1})$. Then, tests were performed to check the unloading check circuit, to ensure that the motor main winding is at a safe voltage level during the measurement of its resistance. Those tests were performed using several compressors of different supply voltages and nominal main winding electrical resistances.

Fig. 5 presents the system behavior immediately after the compressor is shut down. The curve in blue represents the voltage signal measured at the comparator input, and as soon as it falls below the reference voltage the relay which enables the Measuring relays is turned on, as designed. Finally, tests were carried out to check if the protection circuit blocks the measurement if the compressor motor is energized again. In all cases, the relay that controls the supply of the Measurement relays is deactivated just when the main motor winding is energized, as soon as the motor voltage is above the reference voltage, thus proving that the entire protection circuit works as designed.
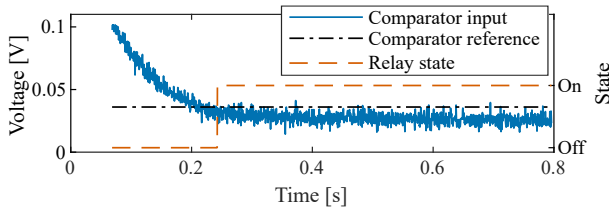


Fig. 5. Test to check the state of the relay that enables the Measuring relays.

## B. Evaluation of Resistance Measurement with and without the Proposed Electronic Board

Tests were performed with three different compressors to evaluate the effect of the proposed protection circuit on the measurement of $R$. For this purpose, the compressors remained for 12 hours in an environment with a temperature controlled at $(23.0\pm0.3)\,°C$ for temperature equalization. Then the value of $R$ for each compressor was measured with and without the proposed electronic board. The first measurement was done with the ohmmeter connected directly to the motor terminal, and the second one considered all the elements of the proposed electronic board in addition to the ohmmeter. Both humidity and temperature were controlled in the room, so their effects on the measurement uncertainty were neglected.

In the case being evaluated in this paper the proposed electronic board is considered in association with the ohmmeter as the measurement chain. The measurement uncertainty for resistance measurements, $O_{\max}$, with the ohmmeter considered in this study (type B uncertainty) in the range of $100\,\Omega$ is given as [22]:

$$O_{\max} = 0.0001R_r + 0.004, \tag{2}$$

where $R_r$ is the reading, in ohms. The smallest range was used in all cases ($100\,\Omega$). Besides the instrumentation uncertainty, the repeatability of measurements was considered (type A

standard uncertainty), represented by the standard deviation of the measurements under the same conditions ($\sigma_R$). For the determination of the measurement uncertainty of $R$, the distribution of the instrumental uncertainty was assumed to be rectangular to minimize the chance of underestimating the actual uncertainty, and the standard deviation was assumed to be normal, since more than fifty consecutive measurements were performed and showed to have a normal-like distribution.

The quantification of the uncertainty of the measurements was done based on the Monte Carlo method (MCM) proposed in [23], which uses the concept of propagation of probability distributions of input quantities, a generalization of the law of propagation of uncertainties [24]. For the specific case of this work, the distribution function of $R$:

$$G_R(\eta) = \int_{-\infty}^{\eta} g_R(z)\mathrm{d}z, \tag{3}$$

is approximated by using the MCM, where $G_R(\eta)$ is the cumulative distribution function of $R$ up to $\eta$ and $g_R(z)$ is the probability density function (PDF) of $R$. In this approach, each measured value, $R$, is obtained as a functional relationship, $\mathrm{f}(\cdot)$, of the input quantities:

$$R = \mathrm{f}(\mathbf{X}), \tag{4}$$

where $\mathbf{X}$ is a vector of the $N$ input quantities $[X_1,\ldots,X_N]^{\mathrm{T}}$. Each input quantity $X_i$ is a random variable with expectation $x_i$ and possible values $\xi_i$. The PDF for the input is denoted as $g_{\mathbf{X}}(\boldsymbol{\xi})$, where $\boldsymbol{\xi} = [\xi_1,\ldots,\xi_N]^{\mathrm{T}}$ is a vector of variables that describe the possible values of $\mathbf{X}$. Since in this study all the input variables are independent, a PDF can be assigned to each input $X_i$ as $g_{x_i}(\xi_i)$, for $i = 1,\ldots,N$. MCM is then used to obtain $M$ model values, $R'_i$ for $i = 1,\ldots,M$, by sampling at random the PDFs for $X_i$ and evaluating f for those values. In this case, the two input PDFs were defined according to the results of type A and type B evaluations of uncertainty. The $M$ resistance values obtained from the $M$ Monte Carlo trials are then ordered into a strictly increasing order to obtain a discrete representation $\mathbf{G}$ of the distribution function $G_R(\eta)$ in (3). The estimate of the output quantity, $\tilde{R}$, is usually obtained from the average of the values in $\mathbf{G}$ as:

$$\tilde{R} = \frac{1}{M} \sum_{i=1}^{M} R'_i. \tag{5}$$

The standard uncertainty is obtained as:

$$u(\tilde{R}) = \sqrt{\frac{1}{M-1} \sum_{i=1}^{M} \left(R'_i - \tilde{R}\right)^2}. \tag{6}$$

Alternatively, it is possible to obtain a coverage interval for a given coverage probability $p$ through the shortest $100p\%$ coverage interval in $\mathbf{G}$. In this study, a coverage probability $p = 95.45\%$ and a number of Monte Carlo trials $M = 10^6$ were considered. Table II presents the estimate of the output, the standard deviation of the measurements, and the resulting uncertainty obtained with the MCM for the coverage probability of $95.45\%$ ($U_{\tilde{R}}$) for each resistance value measured, both for the cases with and without the proposed set of modules.

TABLE II
MEASUREMENT RESULTS WITH AND WITHOUT THE
PROPOSED SET OF MODULES.

| Compressor | Set of modules | $\tilde{R}$ [Ω] | $\sigma_R$ [Ω] | $U_{\tilde{R}}$ [Ω] |
|---|---|---|---|---|
| 1 | Without | 1.277 | 0.002 | 0.005 |
| 1 | With | 1.275 | 0.001 | 0.005 |
| 2 | Without | 5.419 | 0.003 | 0.008 |
| 2 | With | 5.425 | 0.003 | 0.008 |
| 3 | Without | 36.024 | 0.022 | 0.044 |
| 3 | With | 35.999 | 0.025 | 0.050 |

With the results presented in Table II, it is safe to assume the values obtained both using and not using the set of modules can be considered equivalent from the metrological point of view. Therefore, both the measured value and its measurement uncertainty depend only on the ohmmeter used.

As a final step, the measured values of resistance were converted to temperature. For this purpose, the values of $R_0$ [15], for the three compressors, were obtained in a controlled environment at $(20.0 \pm 0.3)\,°C$ using the same ohmmeter described in this section, and their corresponding uncertainties were obtained with the MCM. The results are shown in Table III, which presents the estimate of the main winding temperature, $\tilde{T}$, and the resulting uncertainty obtained with the MCM for the coverage probability of 95.45% ($U_{\tilde{T}}$). Furthermore, Fig. 6 presents a comparison between the uncertainties of the proposed method and works from the literature based on indirect measurements to highlight the improvements obtained.

TABLE III
ESTIMATES OF THE WINDING TEMPERATURES OF THREE
COMPRESSOR MODELS USING THE PROPOSED SET OF
MODULES.

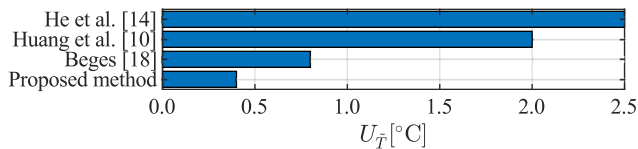| Compressor | $\tilde{T}$ [°C] | $U_{\tilde{T}}$ [°C] |
|---|---|---|
| 1 | 23.1 | 0.4 |
| 2 | 22.9 | 0.3 |
| 3 | 23.0 | 0.3 |



Fig. 6. Comparison between the uncertainties of indirect measurement methods and the proposed method.

### C. Validation of Temperature Estimates against Temperature Measurements

To validate the TRR method against winding temperature measurements, tests were performed using an instrumented compressor. The winding was instrumented in three points, using calibrated Pt100 sensors. The temperature errors in steady state with respect to the mean value of the Pt100 measurements are provided in Fig. 7. For all the four temperature values, the proposed method provides estimates within $\pm 0.15\,°C$ of

the average values of the Pt100 sensors. It is also relevant to mention that the temperature errors have the same order of magnitude of the ones observed in the Pt100 measurements.
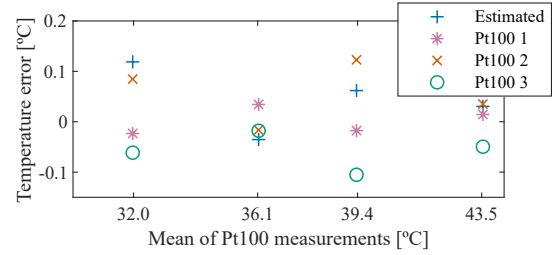


Fig. 7. Temperature error between the Pt100 measurements and the estimated temperature, related to the mean of Pt100 measurements.

## V. CONCLUSION

This paper presents a solution to enable the measurement of the main winding temperature of compressors in quick performance tests automatically and with small uncertainty. The solution is based on the indirect measurement of the temperature by measuring the main winding electrical resistance of the SPIM associated with the refrigeration compressor. A set of modules was designed to automate the measurements and ensure safe operation of the ohmmeter, which must be used right after the motor is switched off and with all auxiliary devices disconnected.

The validation tests showed that the proposed set of modules is capable of automating the measurement of the electrical resistance of the SPIM main winding in a safe way by ensuring that the ohmmeter is connected to the motor only after the voltage over the motor winding is at a safe level. In addition, there are safety layers which ensure that even in the event of a disconnection from the system that controls the activation of the set of modules, there is no risk to the ohmmeter nor to the compressor. Furthermore, the use of the proposed set of modules does not change the measured resistance value, as the observed deviations are smaller than the measurement uncertainty of the ohmmeter used in the tests and are also non-systematic. Thus, the final measurement uncertainty is primarily defined by the uncertainty of the ohmmeter used to measure the resistance of the compressor motor main winding.

The results obtained in this work contribute to the improvement of a method for measuring cooling capacity of refrigeration compressors in a more agile, robust, and metrologically reliable way. As next step, the proposed solution will be evaluated in a pilot project to generate a dataset which allows the assessment of the performance of the inference tools described in [5] with the proposed temperature measurement method. The values of electrical resistance of the main winding of the SPIM may also be used directly as an input in the ANN model, since temperature and resistance are correlated quantities. Furthermore, the solution proposed in this work can be used in other contexts for the measurement of winding resistance or temperature in cases where the measurement must be done with low uncertainty immediately after the motor is turned off, such as fault diagnosis after a forced shutdown. Thus, besides the direct contribution to the performance tests

of refrigeration compressors, this work presents a safe and automatic alternative for the indirect measurement of SPIM winding temperature with low uncertainty.

## ACKNOWLEDGMENT

## REFERENCES

[1] J. M. Belman-Flores, J. M. Barroso-Maldonado, A. P. Rodríguez-Muñoz, and G. Camacho-Vázquez, "Enhancements in domestic refrigeration, approaching a sustainable refrigerator – a review," *Renew. Sust. Energ. Rev.*, vol. 51, pp. 955–968, Nov. 2015. doi:10.1016/j.rser.2015.07.003.

[2] ISO, "ISO 917 - Testing of refrigerant compressors," 1989.

[3] R. Coral, C. A. Flesch, C. A. Penz, and M. R. Borges, "Development of a committee of artificial neural networks for the performance testing of compressors for thermal machines in very reduced times," *Metrol. Meas. Syst.*, vol. 22, pp. 79–88, Mar. 2015. doi:10.1515/mms-2015-0003.

[4] R. C. C. Flesch and J. E. Normey-Rico, "Modelling, identification and control of a calorimeter used for performance evaluation of refrigerant compressors," *Control Eng. Pract.*, vol. 18, pp. 254–261, Mar. 2010. doi:10.1016/j.conengprac.2009.11.003.

[5] R. Coral, C. A. Flesch, and R. C. C. Flesch, "Measurement of refrigeration capacity of compressors with metrological reliability using artificial neural networks," *IEEE Trans. Ind. Electron.*, vol. 66, pp. 9928–9936, Dec. 2019. doi:10.1109/TIE.2019.2898613.

[6] A. L. S. Pacheco, R. C. C. Flesch, C. A. Flesch, L. A. Iervolino, and V. T. Barros, "Tool based on artificial neural networks to obtain cooling capacity of hermetic compressors through tests performed in production lines," *Expert Syst. Appl.*, vol. 194, pp. 116494–116510, May 2022. doi:10.1016/j.eswa.2021.116494.

[7] T. Dutra and C. J. Deschamps, "A simulation approach for hermetic reciprocating compressors including electrical motor modeling," *Int. J. Refrig.*, vol. 59, pp. 168 – 181, Nov. 2015. doi:10.1016/j.ijrefrig.2015.07.023.

[8] A. Nikbakhsh, H. R. Izadfar, and M. Jazaeri, "Classification and comparison of rotor temperature estimation methods of squirrel cage induction motors," *Measurement*, vol. 145, pp. 779 – 802, Oct. 2019. doi:10.1016/j.measurement.2019.03.072.

[9] X. Liang, "Temperature estimation and vibration monitoring for induction motors and the potential application in electrical submersible motors," *Can. J. Electr. Comput. Eng.*, vol. 42, pp. 148–162, Jul. 2019. doi:10.1109/CJECE.2018.2875111.

[10] Y. Huang and C. Gühmann, "Temperature estimation of induction machines based on wireless sensor networks," *J. Sens. Sens. Syst.*, vol. 7, pp. 267–280, Apr. 2018. doi:10.5194/jsss-7-267-2018.

[11] E. Armando, A. Boglietti, F. Mandrile, E. Carpaneto, S. Rubino, and D. G. Nair, "Definition and experimental validation of a second-order thermal model for electrical machines," *IEEE Trans. Ind. Appl.*, vol. 57, pp. 5969–5982, Dec. 2021. doi:10.1109/TIA.2021.3114131.

[12] B. Groschup, M. Nell, F. Pauli, and K. Hameyer, "Characteristic thermal parameters in electric motors: Comparison between induction- and permanent magnet excited machine," *IEEE Trans. Energy Convers.*, vol. 36, pp. 2239–2248, Sept. 2021. doi:10.1109/TEC.2021.3056771.

[13] M. O. Sonnaillon, G. Bisheimer, C. De Angelo, and G. O. García, "Online sensorless induction motor temperature monitoring," *IEEE Trans. Energy Convers.*, vol. 25, pp. 273–280, Mar. 2010. doi:10.1109/TEC.2010.2042220.

[14] L. He, S. Cheng, Y. Du, R. G. Harley, and T. G. Habetler, "Stator temperature estimation of direct-torque-controlled induction machines via active flux or torque injection," *IEEE Trans. Power Electron.*, vol. 30, pp. 888–899, Feb. 2015. doi:10.1109/TPEL.2014.2310902.

[15] IEEE, "IEEE 112 - IEEE standard test procedure for polyphase induction motors and generators," 2017.

[16] R. McElveen, M. Melfi, and J. McFarland, "Improved characterization of polyphase induction motor losses: Test standards must be modified to improve efficiency optimization," *IEEE Ind. Appl. Mag.*, vol. 25, pp. 61–68, Dec. 2019. doi:10.1109/MIAS.2018.2875208.

[17] R. F. McElveen and C. A. Stockton, "Stator winding temperature rise testing for medium and large polyphase induction motors investigated," in *2019 IEEE Petroleum and Chemical Industry Conference (PCIC)*, pp. 83–92, Sept. 2019. doi:10.1109/PCIC30934.2019.9074541.

[18] G. Beges, "Influence of resistance method on motor winding temperature rise measurement," *Int. J. Thermophys.*, vol. 32, pp. 2333–2342, Oct. 2011. doi:10.1007/s10765-011-1121-9.

[19] M. C. Diniz, C. Melo, and C. J. Deschamps, "Experimental performance assessment of a hermetic reciprocating compressor operating in a household refrigerator under on–off cycling conditions," *Int. J. Refrig.*, vol. 88, pp. 587–598, Apr. 2018. doi:10.1016/j.ijrefrig.2018.03.024.

[20] Y. Xia, Y. Han, Y. Xu, and M. Ai, "Analyzing temperature rise and fluid flow of high-power-density and high-voltage induction motor in the starting process," *IEEE Access*, vol. 7, pp. 35588–35595, Mar. 2019. doi:10.1109/ACCESS.2019.2899346.

[21] E. R. Summers, "Determination of temperature rise of induction motors," *Electr. Eng.*, vol. 58, pp. 459–467, Sept. 1939. doi:10.1109/EE.1939.6431520.

[22] Keysight Technologies, *Keysight 34970A - Data Acquisition/Switch Unit Family*, 2014.

[23] JCGM, "Uncertainty of measurement — part 3: Guide to the expression of uncertainty in measurement (GUM:1995). Supplement 1: Propagation of distributions using a Monte Carlo method," 2008.

[24] M. G. Cox and B. R. L. Siebert, "The use of a Monte Carlo method for evaluating uncertainty and expanded uncertainty," *Metrologia*, vol. 43, pp. S178–S188, Aug. 2006. doi:10.1088/0026-1394/43/4/S03.

**Murilo Ferreira Vitor** received a B.E. degree in control and automation engineering and the M.Eng. degree in mechanical engineering from the Federal University of Santa Catarina (UFSC), Florianópolis, Brazil, in 2016 and 2019, respectively. He is currently pursuing his Ph.D. in automation and systems engineering at UFSC, and his main research interests include applied artificial intelligence, instrumentation, and control and automation of tests.

**João Paulo Zomer Machado** received a B.E. degree in control and automation engineering at the Federal University of Santa Catarina (UFSC), Florianópolis, Brazil in 2020. He is currently pursuing a master's degree in automation and systems engineering at UFSC, and his main research interests include applied artificial intelligence, instrumentation, and automation of tests.

**Antonio Luiz Schalata Pacheco** received a B.S. degree in mathematics, a M.Sc. in scientific and industrial metrology and a Dr.Eng. in mechanical engineering at the Federal University of Santa Catarina (UFSC), Florianópolis, Brazil, in 2003, 2007, and 2015, respectively. Currently, he is conducting development activities at the Institute of Power Electronics, Department of Electrical and Electronic Engineering, UFSC, Brazil, and his main research interests are applied artificial intelligence, automation of tests, and development of measurement systems.

**Rodolfo César Costa Flesch** received the B.E., M.Eng., and Dr.Eng. degrees in control and automation engineering from the Federal University of Santa Catarina (UFSC), Florianópolis, Brazil, in 2006, 2009, and 2012, respectively. He is currently a professor at the Department of Automation and Systems Engineering, UFSC, and a researcher with the Brazilian National Council for Scientific and Technological Development, Brasília, Brazil. In addition, he is the coordinator of several R&D cooperation projects between academia and industry. His current research interests include process control (time-delay processes and model predictive control), instrumentation, and automation of tests.